Lorentz Force Effects in Multimodality MR-SPECT Imaging

M. J. Hamamura[1], S-H. Ha[1], W. W. Roeck[1], O. Nalcioglu[1], D. J. Wagenaar[2], D. Meier[2], and B. E. Patt[2]

[1]Tu & Yuen Center for Functional Onco-Imaging, University of California, Irvine, CA, United States, [2]Gamma Medica-Ideas Inc., Northridge, CA, United States

Purpose

A significant challenge in the development of a multimodality MR-SPECT system is ensuring that the MRI and SPECT hardware are compatible with each other. Cadmium-zinc-telluride (CZT) semiconductor detectors are capable of operating in high magnetic fields [Wagenaar D *et al*, IEEE Nuc Sci Symp Conf Rec 1825-8 (2006)]. However, electron-hole pairs created by the interaction of incoming gammy rays are subject to the Lorentz force. As a result, when a detector is placed in any orientation other than aligned with the static magnetic field of the MRI system, electrons traveling towards the anode will experience a shift in their detected position. In this study, we investigated the effects of this Lorentz force.

Methods

For the test phantom, a hollow cylinder with an inner diameter of 16 mm and length of 45 mm was filled with a Tc-99m / $CuSO_4$ solution. A centrally located solid acrylic rod (cold spot) with a diameter of 6 mm was placed within this cylinder. The phantom was placed in the center of a custom RF birdcage coil, in which the separation between two rungs was opened to allow for the insertion of a lead parallel-hole collimator. The collimator was positioned next to a CZT detector unit on one end, and fixed 5 mm from the test phantom on the opposite end. The CZT detector measures 2.54 x 2.54 x 0.5 cm and consists of 16 x 16 pixels (1.59 mm pitch). The CZT detector/RF coil/phantom setup was placed into a 4 T MRI system, as diagramed in Fig. 1.

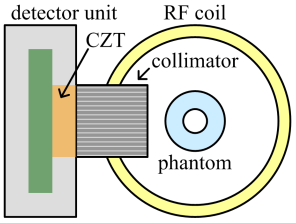

Fig. 1. *MR-SPECT setup*

An MR image was acquired using a 2D spin-echo pulse sequence with the following parameters: TR = 500 ms, TE = 20 ms, FOV = 50 mm, matrix = 256X256, slice thickness = 5 mm, NEX = 2. 2D projection images were acquired using a 10% energy window around the 140 keV photopeak. As is standard for nuclear imaging systems, a flood field image was acquired to correct for spatial variations in the sensitivity. As illustrated in Fig. 2, detected electrons experienced a shift in the –x direction due to the effects of the Lorentz force. For comparison, projection images and a flood field image were also acquired with the CZT detector/phantom unit placed away from the MRI system (@ 0 T).

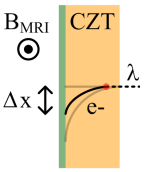

Fig. 2. *Lorentz force effect*

Projection data corresponding to the co-registered MRI slice were used in the SPECT reconstruction. Since we used a rotationally symmetric phantom, it was assumed that all angular views would be identical. The single projection data was thus used for 32 equally spaced views around 360 degrees. Filtered-back-projection with the Shepp-Logan filter was performed on these data, and the resulting reconstructed SPECT images were interpolated to the same field-of-view (FOV) and matrix as the MR images for direct comparison.

Results

Profiles for 3 different sets of projection data corresponding to the MRI slice are shown in Fig. 3. Sensitivity correction of the SPECT data acquired outside the MRI was performed using the flood field image acquired outside the MRI (OUT-OUT). Sensitivity correction of the SPECT data acquired within the MRI was performed using either the flood field image acquired within the MRI (IN-IN) or outside the MRI (IN-OUT). From comparison of the profiles of IN-IN and OUT-OUT, a shift in the phantom position of approximately -1.5 mm was observed. A 4th projection data set (IN-IN-SHIFT) was generated by shifting IN-IN +1.5 mm back to its proper location. The MR and reconstructed SPECT images of these 4 data sets are shown in Fig. 4. The profiles of these images along the horizontal diameter are shown in Fig. 5. For further discussion, the absolute difference of the flood field image acquired outside the MRI and the flood field image acquired inside the MRI and shifted by +1.5 mm is given in Fig. 6.

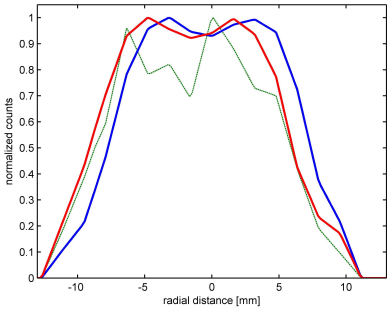

Fig. 3. *Projection profiles for OUT-OUT (blue), IN-IN (red), and IN-OUT (green).*

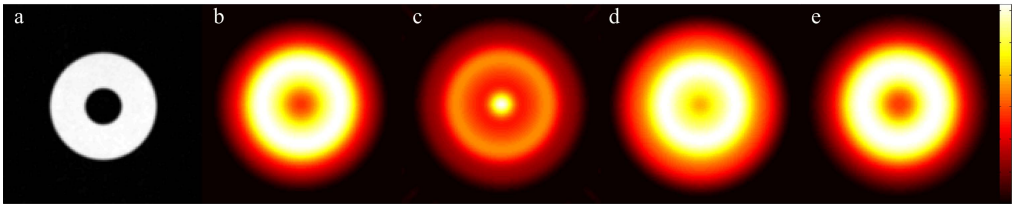

Fig. 4. *(a) MRI and SPECT images of (b) OUT-OUT, (c) IN-OUT, (d) IN-IN, and (e) IN-IN-SHIFT*

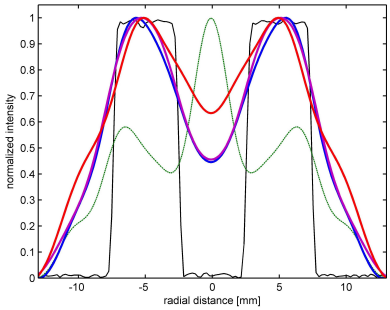

Fig. 5. *Reconstruction profiles for MRI (black), OUT-OUT (blue), IN-IN-SHIFT (purple),IN-IN (red), and IN-OUT (green).*

Discussion

The results demonstrate that the Lorentz force generates measurable effects that must be taken into account when performing MR-SPECT imaging. Failure to account for the apparent shift in object position results in a degradation of the SPECT reconstruction, as seen in Figs. 4, and 5. Furthermore, sensitivity correction of data acquired within a MRI must be performed using flood field images also acquired within the MRI at the appropriate location. As seen from the nonzero values in Fig. 6, it is insufficient to acquire flood field data outside the MRI and simply shift the position of the resulting image. Unlike the moving electrons, the physical imperfections in the detector unit that cause the non-uniform sensitivity are fixed and do not shift in position.

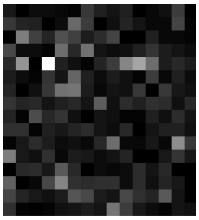

Fig. 6. *Difference in flood field images*

Any centrally facing detector located within a plane whose normal is parallel to the main static MRI field experiences the same amount of Lorentz force shift in the acquired data. As a result, a single flood field image taken at one of these positions can be used to correct for data acquired at any of these positions. However, data acquired at a detector position outside this plane must be corrected using a separate flood field image acquired at the appropriate location. For the (two) orientations where the detector is parallel with the MRI field, the Lorentz force goes to zero. In summary, it is imperative that the appropriate flood field image be used to correct projection data and that the apparent shift in object position be taken into account during the reconstruction process.

This research is supported in part by CIRM training grant T1-00008 (for S. Ha) and NIH NIBIB grant R44EB006712.